Schweizerischer Erdbebendienst
Service Sismologique Suisse
Servizio Sismico Svizzero
Swiss Seismological Service

ETH zürich

The new BBToolbox 2.0: a revised tool to compute hybrid synthetic seismograms

W. Imperatori[1], D. Fäh[2]

[1]Swiss Seismological Service (SED), ETH Zurich, Switzerland. Email: walter.imperatori@sed.ethz.ch
[2]Swiss Seismological Service (SED), ETH Zurich, Switzerland, Email: donat.faeh@sed.ethz.ch

1) Introduction

Broadband simulation methodologies represent a valuable tool to provide fast estimates of the ground shaking expected during future earthquakes. In standard practice, ground-motion intensities are typically evaluated in terms of scalar values (e.g. PGA) derived from ground motion prediction equations. However, the possibility to have reliable near-source synthetic time-series spanning a wide range of frequencies is highly appealing to the seismic engineering community as it allows more refined structural analysis of sensible infrastructures.

2) Background

We present a new, improved version of the hybrid broadband technique originally developed by Mai et al. (2010). In their version, the high-frequency part was based purely on the multiple S-to-S scattering model of Zeng et al. (1991). Scattering was assumed to originate simply at the hypocenter of the earthquake. However, such approximation does not hold for large fault ruptures, especially in the near-fault region.

In our version, the high-frequency part has two components: a deterministic one, based on a ray-theory technique (Spudich and Frazer, 1984), and a stochastic one, represented by the multiple S- to-S scattering model of Zeng et al. (1991).

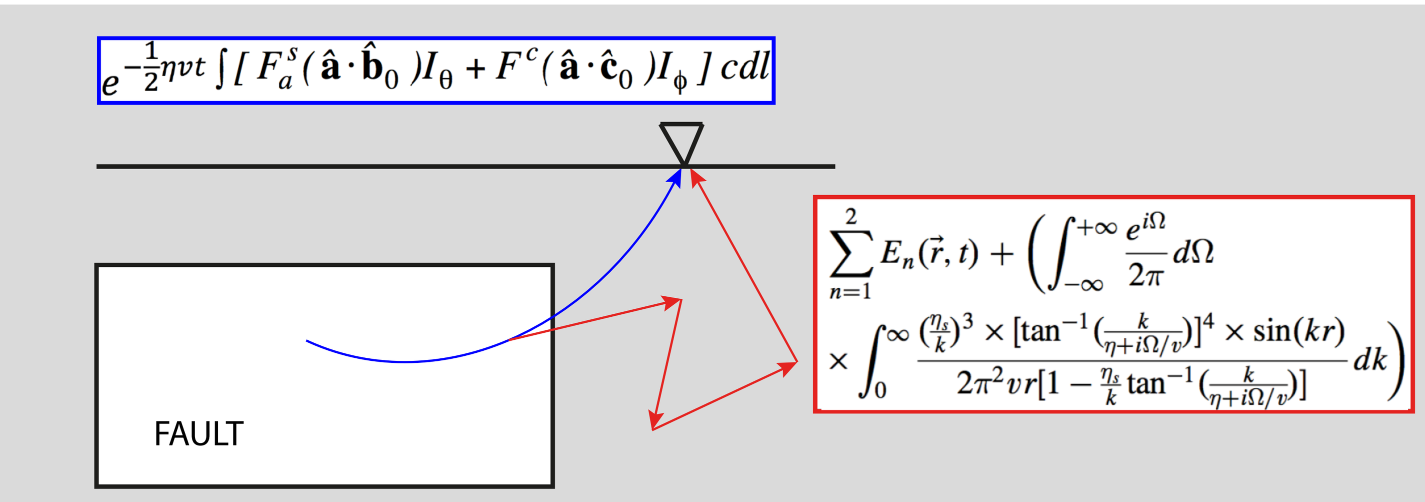

Figure 1. Sketch illustrating the double nature of the high-frequency radiation (S-waves case): deterministic (in blue) and stochastic (in red). The deterministic component (obtained by calculating surfaces integrals on the fault plane) is attenuated by the frequency-dependent exponential term. The energy lost by scattering is transferred to the stochastic component, whose envelope is controlled by the multiple S-to-S scattering model (red box).

Scattering attenuation controls the amount energy transferred from the deterministic component to the stochastic one. On the other hand, intrinsic attenuation is based on a power-law model (Müller, 1983) accounting for dispersion. This power-law is applied to both the deterministic waves and the contribution of each randomly distributed scatterer (shaped by the envelope predicted by Zeng et al. scattering model).

In general, while the deterministic component dominates towards the matching frequency (i.e. the point where low-frequency and high-frequency synthetics are reconciled), the stochastic part takes over as frequency increases (see figure 2). This transition is mainly controlled by the total attenuation and the source-receiver distance.

2) Point-source

To test the accuracy of the deterministic high-frequency module of our code, we consider a point-source embedded in an homogeneous, elastic half-space. Reference seismograms are computed with a 4-th order finite difference code up to 5Hz.

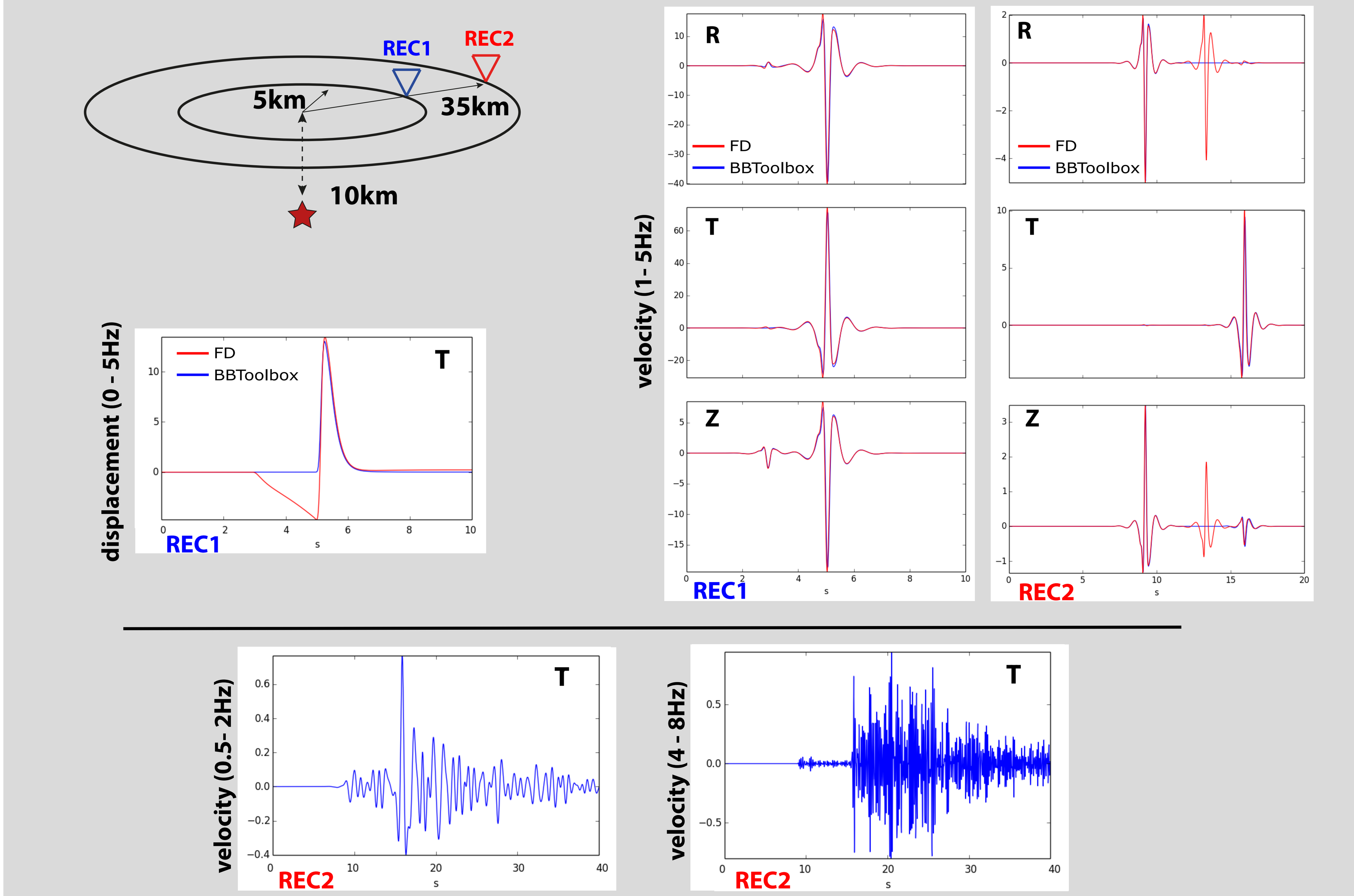

*Figure 2. **Top**: comparison between synthetic seismograms computed using our code (in blue) and a finite-difference (FD) code (in red). Note the presence of an evanescent P-wave for receiver 2 in the FD solution. Bottom left: displacement on the transversal component for receiver 1, evidencing the near-field motion missing in our solution. **Bottom**: synthetics at two different frequency bands for receiver 2, this time including scattering attenuation.*

4) Extended Source

Our version implements a substantial set of advanced features. For instance, the user can specify a low-resolution slip model and the code generates automatically a high-resolution rupture model providing stable omega-squared spectral decay at high-frequency and frequency-dependent directivity effect (Gallovic, 2015). Fractal non-planarity, leading to local variations of strike, dip and rake, can be added automatically.

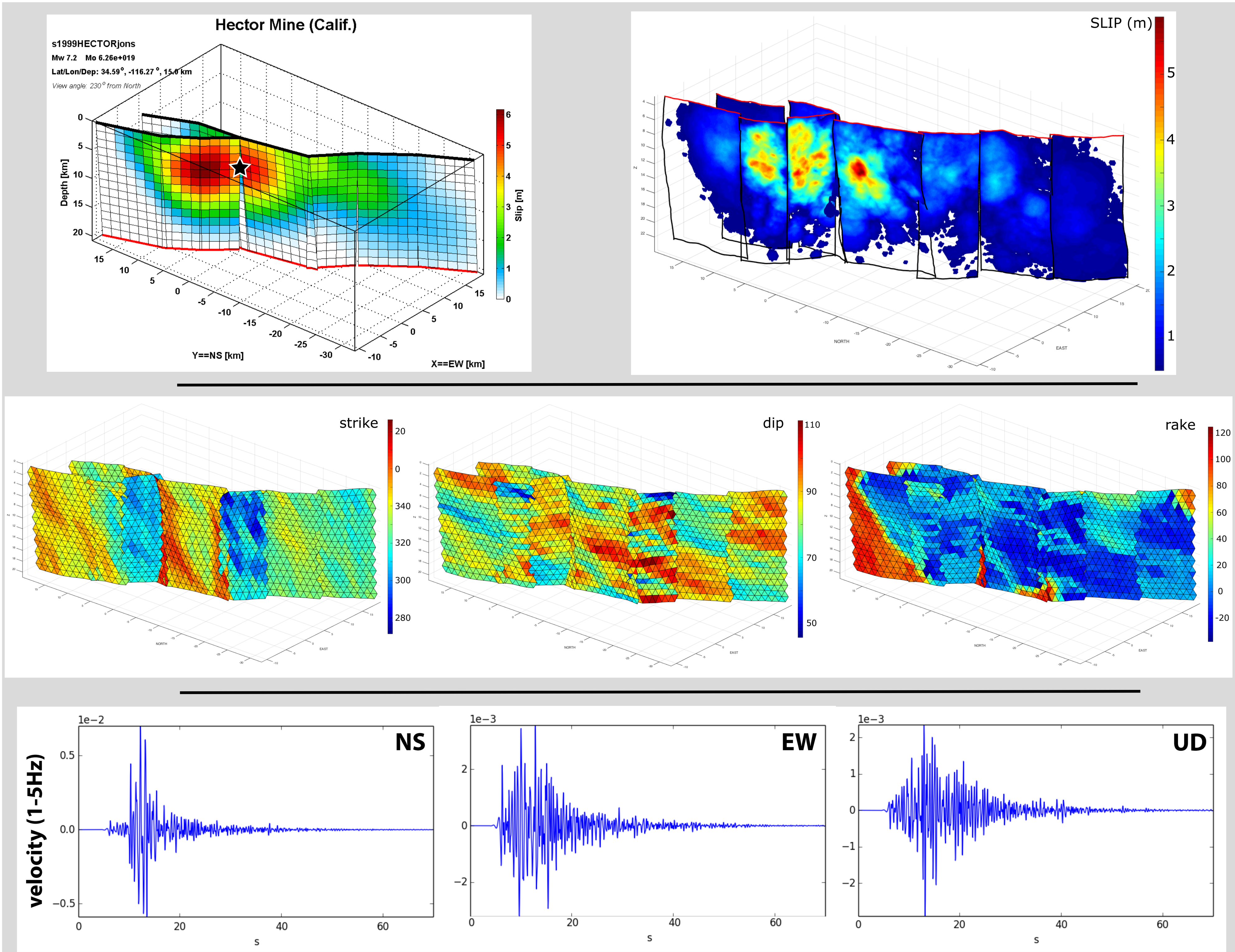

*Figure 3. **Top**: input low-resolution (left) and high-resolution slip model (right). **Middle**: strike, dip and rake after fault roughness has been added (a low-resolution mesh is shown). **Bottom**: sample synthetics in the 1-5Hz frequency range (no low-frequency component).*

5) Next Steps

- Complete the implementation of new features and further testing by comparison with finite-difference results.
- We plan to extend our methodology to correctly generate broadband synthetics also at depth. This will make our code a valuable tool in seismic hazard assessment for underground nuclear waste repositories.
- Careful calibration of the parameters controlling the scattering model based on observed and synthetic data. Although regional relationships for intrinsic and scattering Q are available, we anticipate that station-specific estimates are fundamental for realistic modeling of high-frequency waveforms.
- Full validation by comparing synthetics to strong-motion recordings.

References

Mai, P.M., Imperatori, W., Olsen, K.B., P.M. (2010). Hybrid Broadband Ground-Motion Simulations: Combining Long-Period Deterministic Synthetics with High-Frequency Multiple S-to-S Backscattering, BSSA, doi: 110.1785/0120080194.

Gallovič, F. (2015). Modeling velocity recordings of the Mw6.0 South Napa, California, earthquake: unilateral event with weak frequency directivity, SRL, doi: 10.1785/0220150042.

Müller, G. (1983). Rheological properties and velocity dispersion of a medium with power-law dependence of Q on frequency, J. of Geophysics, 54:20-29

Spudich, P., Frazer, L.N. (1984). Use of ray theory to calculate high-frequency radiation from earthquake sources having spatially-variable rupture velocity and stress drop, BSSA, 74 (6).

Zeng, Y., Su, F., Aki, K. (1991). ScatteringWave EnergyPropagationin a RandomIsotropic Scattering Medium: Theory, JGR, 96 (B1).

Acknowledgment

This research has been founded through a contract with the Swiss Federal Nuclear Safety Inspectorate (ENSI).